

Autonomous Robot Navigation for Precision Horticulture

T. Hague J. A. Marchant N. D. Tillett
Silsoe Research Institute
Wrest Park, Silsoe, U.K.

Abstract

Certain experimental horticultural operations require an autonomous vehicle capable of navigating through a field of crop plants. An image analysis system exists which can locate the crop row structure, but simple reactive control of the vehicle on the basis of this data would not be sufficiently reliable; instead a multi-sensor data fusion based approach is preferred. Since the vehicle must be able to operate in many fields to be economic, artificial navigation beacons and detailed prior maps are disadvantageous.

A novel navigation scheme has been devised, which allows the crop rows themselves to be used as a navigation aid. The commanded path of the vehicle through the field is expressed by path curvature as a function of forward distance; parts of the path are marked as being aligned with crop rows. Data from image analysis is combined with that from a solid state compass and dead reckoning using an extended Kalman filter. Rather than position in an arbitrary cartesian coordinate frame, the EKF estimates position and orientation error from the commanded path, which may be used directly for feedback control of vehicle motion.

The method has been implemented on a small horticultural vehicle, allowing it to follow crop rows and turn at the end of the rows fully autonomously. The system has been tested in the field, and results showing the accuracy of guidance along crop rows are presented.

1 Introduction

Current research at Silsoe Research Institute is concerned with the application of agro-chemical treatments - e.g. herbicides, pesticides or foliar feeds, on a selective basis to individual crop plants or weeds. It is thought that by this approach, chemical inputs may be reduced by perhaps 80%, with obvious environmental

benefits.

The implementation of this approach uses an image analysis system to locate and identify plants, weeds and soil in real time from views taken from a camera ahead of the spray bar [2]. A continuous local map is formed by merging the data from individual images, and the contents of this map are then used to determine whether treatment should be applied by each of a closely spaced array of spray nozzles.

As a result of the required precision and the consequent complexity of the applicator, the large boom widths used in conventional crop spraying are impractical. The need to identify and differentiate between crop plant and weeds in real time, combined with physical limitations on the time needed to turn on and off a spray jet, place an upper limit on vehicle forward speed in the region of 1ms^{-1} . Taken together, these constraints place a limit on the rate of work making it impractical to perform such precision operations from a manually driven vehicle. For this reason a totally automated solution has been sought. This requires an autonomous vehicle which can follow rows of crop plants; moreover, it must detect when the end of the row has been reached, and relocate itself at the head of the next row, continuing until the whole plot has been treated.

2 Navigation and guidance

A now conventional guidance strategy for robot vehicles is to solve the *localisation* problem by fusion of dead reckoning information and observations of fixed beacons or landmarks, e.g. [4]. An extended Kalman filter is typically used to maintain an estimate of position in some chosen cartesian world coordinate frame. The desired paths for the vehicle are also expressed in this coordinate system, allowing the positional errors to be computed.

For the horticultural application, sections of the

path are determined by the position of the plant rows, which it would be impractical to map *a priori* in a cartesian coordinate frame; instead the plant rows must be located on-line. An attractively simple approach would be to use a sensor based control system where the detected locations of crop plants given by the image analysis system are used to allow the vehicle to follow the rows, in much the way that the basic industrial AGV follows a leader cable. The limitation with this approach is that of robustness: the sensor data is of rather poor quality; plants may be missing in areas. Also, the vehicle must be able to turn automatically when the end of the row is reached.

For the horticultural robot, the robustness benefits of a system based upon multi sensor fusion are desirable without the need for artificial beacons or a detailed *a priori* map of the field. We have achieved this by using a novel method for specifying commanded paths and vehicle position. The commanded trajectory of the vehicle is expressed by the curvature of the path $c(x)$ and the commanded speed $v(x)$ as functions of distance traveled, x . The path is split into segments, such that $c(x)$ and $v(x)$ are piecewise linear functions. Some of the segments are associated with crop rows; these are labeled as such in the path description, and assumed to be nominally straight. For the turning manoeuvres, a collection of segments are assembled which yield a 180° turn suitable for the (known) spacing of the crop rows.

Vehicle position may be expressed with respect to the commanded path in an intrinsic coordinate set $[x\ y\ \theta]$, where x is the forward distance along the path, y the perpendicular offset, and θ the orientation of the vehicle relative to the tangent direction of the path at that point. Thus we estimate directly state variables y and θ , which are the position and orientation errors needed to control the vehicle steering, without the intermediate step of obtaining position in a cartesian coordinate frame.

3 EKF position estimator formulation

The position of the vehicle, in the form given above, is estimated using an extended Kalman filter (EKF) [1]. The linear (v) and angular (Ω) speeds which are provided by the vehicle low level control system are used in the prediction step.

Observations of offset and heading angle relative to the plant rows are provided by an image analysis system (fully described elsewhere [5]), and vehicle orientation is measured by a solid state magnetic compass.

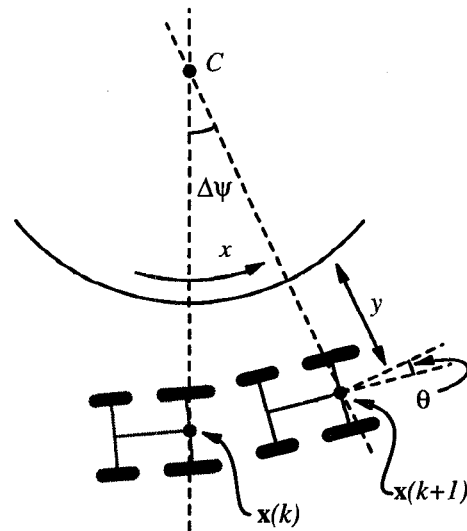


Figure 1: Vehicle position when following a curved path segment.

The EKF formulation described here is a development of the method described in [3].

3.1 Plant model

Let the system state at time k be represented by the vector $\mathbf{x}(k) = [x(k)\ y(k)\ \theta(k)\ \psi(k)]^T$, where $x(k), y(k), \theta(k)$ denote the vehicle position relative to the demanded path. State variable $\psi(k)$ is the angle in the horizontal plane between the tangent direction of the path and magnetic north, and is used in interpreting compass observations.

The plant is modelled by the non-linear discrete time state transition equation

$$\mathbf{x}(k+1) = \mathbf{f}(\mathbf{x}(k), \mathbf{u}(k)) + \mathbf{v}(k) \quad (1)$$

where $\mathbf{u}(k) = [v\ \Omega]^T$ and $\mathbf{v}(k)$ represents zero mean plant noise.

As the vehicle follows a curved path, in time step τ the small incremental motion from position $\mathbf{x}(k)$ to $\mathbf{x}(k+1)$ subtends angle $\Delta\psi$ about the centre of curvature C of the demanded path as shown in figure 1. Approximating curvature $c(x)$ as constant, and the vehicle motion as a translation of distance τv in the direction the vehicle is oriented, it can be shown by geometric considerations that

$$\Delta\psi = \tan^{-1} \left[\frac{\tau v c(x) \cos \theta}{1 - c(x)(y + \tau v \sin \theta)} \right] \quad (2)$$

and

$$\mathbf{f}(\mathbf{x}(k), \mathbf{u}(k)) = \begin{bmatrix} x(k) + \frac{\Delta\psi}{c(x(k))} \\ y(k) + \tau v (\sin \theta - \cos \theta \tan \frac{\Delta\psi}{2}) \\ \theta(k) + \tau\Omega - \Delta\psi \\ \psi(k) + \Delta\psi \end{bmatrix} \quad (3)$$

Equation (3) is used as the plant model when the commanded path curvature is non-zero. However, (3) cannot be evaluated when path curvature $c(x)$ is small. In the limit as $c(x) \rightarrow 0$, (2) and (3) reduce to

$$\mathbf{f}(\mathbf{x}(k), \mathbf{u}(k)) = \begin{bmatrix} x(k) + \tau v \cos \theta(k) \\ y(k) + \tau v \sin \theta(k) \\ \theta(k) + \tau\Omega \\ \psi(k) \end{bmatrix} \quad (4)$$

which is the familiar form used for localisation in a cartesian coordinate frame. This reduced form is used as the plant model in place of (3) when following a straight path (i.e., $c(x) = 0$).

3.2 Observation models

Two sensor systems are used to correct the position estimates, a solid state magnetic compass, and the image analysis system.

The magnetic compass used is a three axis solid state magnetometer. To simplify the data fusion problem, the 3D measurement is projected onto the horizontal using measured vehicle pitch and roll angles, to give a single heading (yaw) measure. The magnetometer data has an additional complication; the presence of steelwork in the structure of the vehicle distorts the heading data. This effect is first compensated for using a look up table, built by recording compass data against true orientation whilst the vehicle is driven in circles. A 64 element look up table is used, with linear interpolation applied to obtain intermediate points. The corrected single element observation $\mathbf{z}_1(k)$ has observation model:

$$\mathbf{z}_1(k) = \mathbf{h}_1(\mathbf{x}(k)) + \mathbf{w}_1(k) \quad (5)$$

where

$$\mathbf{h}_1(\mathbf{x}(k)) = [\theta(k) + \psi(k)] \quad (6)$$

Noise input $\mathbf{w}_1(k)$ is modelled as Gaussian; this is technically rather inaccurate but in practice adequate.

The image analysis system exploits the heightened contrast between plant matter and the soil background in near infra-red images to locate plants by applying an (automatically computed) amplitude threshold. A Hough transform technique is then applied to locate the underlying row structure. The observations derived by image analysis are $\mathbf{z}_2(k) = [y_2(k) \theta_2(k)]^T$, the

lateral offset and orientation of the camera relative to the plant row. The corresponding observation model explains the location of the camera on the vehicle, a distance T_x ahead of the vehicle reference location:

$$\mathbf{z}_2(k) = \mathbf{h}_2(\mathbf{x}(k)) + \mathbf{w}_2(k) \quad (7)$$

where

$$\mathbf{h}_2(\mathbf{x}(k)) = \begin{bmatrix} y(k) + T_x \sin \theta(k) \\ \theta(k) \end{bmatrix} \quad (8)$$

where $\mathbf{w}_2(k)$ represents a noise input. A major component of the noise input arises from the natural variability of the growth habit of the plants, and a Gaussian model is not an unreasonable approximation.

3.3 EKF implementation

As both the plant model and observation model for the image analysis observations are non-linear, a first order extended Kalman filter is used. Let $\hat{\mathbf{x}}(k|k)$ be the state estimate at time k based on sensor observations up to and including time k . One step prediction of state estimate $\hat{\mathbf{x}}(k+1|k)$ is made using (3), or (4) if the path curvature is small (in practice, less than $\pm 10^{-3} m^{-1}$ is considered "small"). The computation of covariance $\mathbf{P}(k+1|k)$ is simplified by the assumption that the dominant source of noise input $\mathbf{v}(k)$ in the state prediction is from error in the speed measures $\mathbf{u}(k)$, hence

$$\mathbf{P}(k+1|k) = \mathbf{F}_x \mathbf{P}(k|k) \mathbf{F}_x^T + \mathbf{F}_u \mathbf{Q}(k) \mathbf{F}_u^T \quad (9)$$

where

$$\mathbf{F}_x = \frac{\partial \mathbf{f}}{\partial \mathbf{x}}, \quad \mathbf{F}_u = \frac{\partial \mathbf{f}}{\partial \mathbf{u}}$$

These partial derivatives may be evaluated when curvature function $c(x) = ax + b$ where a, b are constants; these are clothoid curves, and are the form in which all path segments for the vehicle are specified (including the degenerate forms where $a = 0$, i.e., straight lines and circular arcs). Paths constructed from clothoids are useful as they can be formed so that the curvature of the path is a continuous function of distance; this ensures smooth motion of the vehicle and reduces the extent of wheel slippage. Whilst clothoid curves are inconvenient to use in a cartesian coordinate system (where there is no general analytic form for the curve), they are the natural choice in the coordinate system we have adopted. Covariance matrix $\mathbf{Q}(k)$ associated with speed vector $\mathbf{u}(k)$ is provided by the vehicle low level control system.

Magnetometer observations $\mathbf{z}_1(k)$ are available at the full rate at which predictions are made using the

plant model (50 per second). The computationally intensive nature of the algorithms limits image analysis observations $\mathbf{z}_2(k)$ to 10 per second, and observations cannot be derived if insufficient plants are in view, including during turning manoeuvres at the end of rows.

Correction of the state prediction $\hat{\mathbf{x}}(k+1|k)$ is thus performed either using magnetometer data alone, or with observations from both sensor systems combined. This can be performed using the normal formulation for a first order EKF, with observation vector $\mathbf{z}(k+1)$ and observation model $\mathbf{h}(\cdot)$ equal to $\mathbf{z}_1(k+1)$ and $\mathbf{h}_1(\cdot)$ respectively (magnetometer reading only) or formed by stacking observations and observation models when image analysis data is also available.

In either case the predicted measurement takes the form

$$\hat{\mathbf{z}}(k+1|k) = \mathbf{h}(\hat{\mathbf{x}}(k+1|k)) \quad (10)$$

with measurement prediction covariance

$$\mathbf{S}(k+1) = \mathbf{H}\mathbf{P}(k+1|k)\mathbf{H}^T + \mathbf{R} \quad (11)$$

where

$$\mathbf{H} = \frac{\partial \mathbf{h}}{\partial \mathbf{x}}$$

The covariances \mathbf{R} used are constant, and are pessimistically chosen on the basis of experimental data.

The Kalman gain $\mathbf{W}(k+1)$, corrected state estimate $\hat{\mathbf{x}}(k+1|k+1)$ and covariance $\mathbf{P}(k+1|k+1)$ are computed using the standard Kalman filter equations

$$\mathbf{W}(k+1) = \mathbf{P}(k+1|k)\mathbf{H}^T\mathbf{S}^{-1}(k+1) \quad (12)$$

$$\hat{\mathbf{x}}(k+1|k+1) = \hat{\mathbf{x}}(k+1|k) + \mathbf{W}(k+1)(\mathbf{z}(k+1) - \hat{\mathbf{z}}(k+1|k)) \quad (13)$$

$$\mathbf{P}(k+1|k+1) = \mathbf{P}(k+1|k) - \mathbf{W}(k+1)\mathbf{S}(k+1)\mathbf{W}^T(k+1) \quad (14)$$

A convenient alternative implementation is possible by noting that the correction step of the EKF (equations 10...14) is a recursive least-squares estimator, and since the observation noise is uncorrelated between the two sensor systems it is not necessary to stack together the magnetometer and image analysis observations. Instead the two sets of observations can be processed sequentially using (equations 10...14), with the same final result.

4 Headland detection

As mentioned earlier, the path description is composed of a sequence of clothoid segments, some of which are "attached" to crop rows, and others which describe turning manoeuvres to be executed at the *headland*

(the end of the crop row). For the segments comprising these turns, the length of each clothoid segment is contained in the path description. For segments corresponding to crop rows, it would be inconvenient to supply the exact row length; instead an approximate row length and associated expected error is supplied in the path description. The end of the row is automatically detected by the absence of plants in the row positions, at a forward distance which is within the supplied tolerance of the row length. The requirement of an approximate row length statistic avoids premature turns occurring should a small patch of crop be missing.

5 Experimental vehicle

The EKF has been implemented as the state estimator for a small horticultural vehicle, shown in the motion sequence of figure 3(a-f). The machine spans a bed of three rows of crop plants (the width between the wheels is 1.86m). It is powered by a small internal combustion engine, which drives each of the two front wheels via independent continuously variable hydrostatic transmission units, which are electrically actuated under computer control. The vehicle is completely self contained; electrical supplies are derived from an onboard battery/alternator. The maximum speed is 1.8 ms⁻¹.

The control, image analysis and position estimation modules run on a network of transputers. One transputer executes a low level control facility, which provides both control of vehicle speed and supplies speed vector $\mathbf{u}(k)$. The EKF position estimator itself runs on a separate T805 transputer. For development purposes, the transputer network is hosted by a laptop PC, which provides a user interface only.

6 Experimental results

Early experimental trials reported in [3] were conducted on an ideal "simulated" crop (i.e., a dark surface with white disks painted to represent the plants). More recent trials have been performed in the field; figure 2 shows the row following performance in real brassica crop (plants around 100mm height). As mentioned earlier, the vehicle spans a bed of three rows of plants; the plants were spaced at 0.5m (typical for brassica) and arranged on the square (i.e., forming a grid) for this experiment, although this is not a requirement for the vehicle. The forward speed of the vehicle was 0.7ms⁻¹. The lateral offset was measured by affixing a nozzle at the centre of the vehicle; the

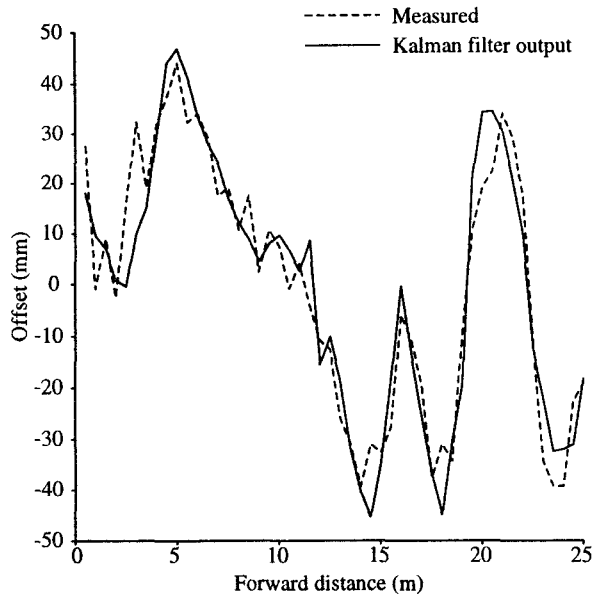


Figure 2: Vehicle offset (y): EKF estimated and manually measured.

location of a trail of paint dispensed from this nozzle was measured relative to the mean position of the three plants at each plant position along the row. The control system was also made to record the estimated offset data from the EKF; manually measured offset is shown alongside the EKF estimated offset at each plant position. The measured RMS positional error of the vehicle from the row position is 21mm . The RMS error between the internal EKF estimate of offset and that measured is just 8mm .

Trials to measure the reliability of the system are yet to be performed; indeed it is difficult to produce a meaningful measure of failure rate since this will depend upon the state of the crop, the soil and lighting conditions etc. However, the vehicle has been operated extensively in a variety of crop circumstances; brassica crops of various stages of growth, planted both manually and with a mechanical transplanter, as well as directly drilled sugar beet plants have been used. Sustained operation on sets of 4 and 8 plant beds of 40m in length (including 3 and 7 headland turns, respectively) has been achieved. The sequence in figure 3(a-f) were taken from a video recording of the vehicle executing a set of 4 passes. A headland turn is shown; note that the spacing of the plant beds demands a tight turn, causing the inside wheel to be driven in reverse during parts of the turn.

7 Conclusions

A navigation method has been devised for an autonomous horticultural robot, which allows the benefits of a multi-sensor data fusion based system to be exploited without need for a cartesian world coordinate frame, or a prior map of the environment. Instead only a path description embodying approximate row lengths and spacings is required *a priori*. The crop rows themselves provide a sufficient navigational aid, obviating the need for artificial beacons.

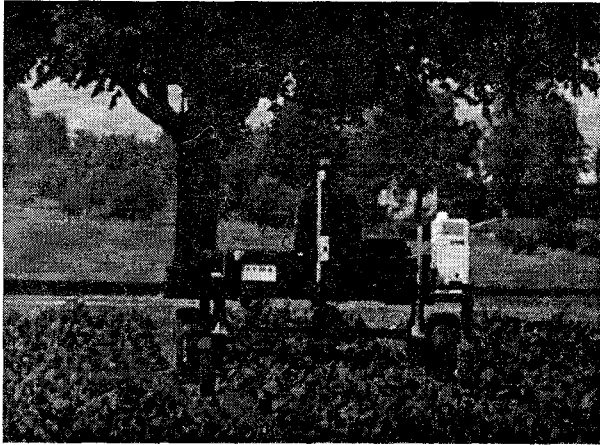
The performance illustrated in figure 2 shows that the crop rows can be followed with a standard error of 21mm . However, by comparison of the manually measured and EKF estimated lateral offset, it may be seen that the position estimation more accurate - 8mm being the standard error between the two; this indicates that the greatest source of inaccuracy in row following arises in the control of the vehicle rather than the state estimation.

Formal trials of reliability remain an area for future work, although sustained operation for sets of 4 and 8 plant beds connected by automatic turns at the end of each row have been achieved without failure.

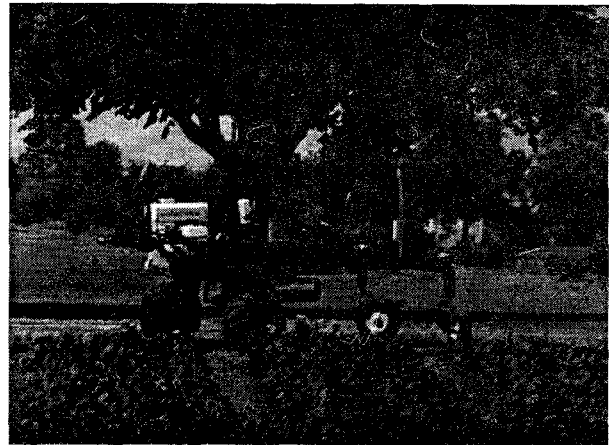
Acknowledgements - This work was supported by the Biotechnology and Biological Sciences Research Council and the Douglas Bomford trust.

References

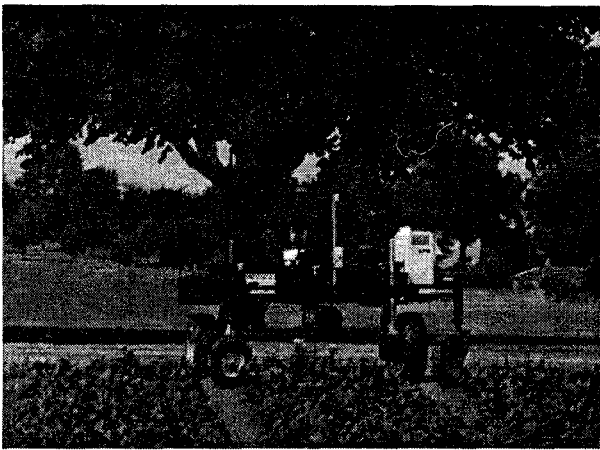
- [1] Y. Bar-Shalom and T. Fortmann. *Tracking and Data Association*. Academic Press, New York, 1988.
- [2] R. Brivot and J. A. Marchant. Segmentation of plants and weeds using infrared images. *Proceedings of the IEE - Vision, Image and Signal Processing*. In Press.
- [3] T. Hague and N. D. Tillett. Navigation and control of an autonomous horticultural robot. *Mechatronics*, 6(2):165-180, March 1996.
- [4] J. J. Leonard and H. F. Durrant-Whyte. Mobile robot localisation by tracking geometric beacons. *IEEE Trans. Robotics and Automation*, 7(3):376-382, June 1991.
- [5] J. A. Marchant and R. Brivot. Real time tracking of plant rows using a Hough transform. *J. Real Time Imaging*, 5(1), 1995.



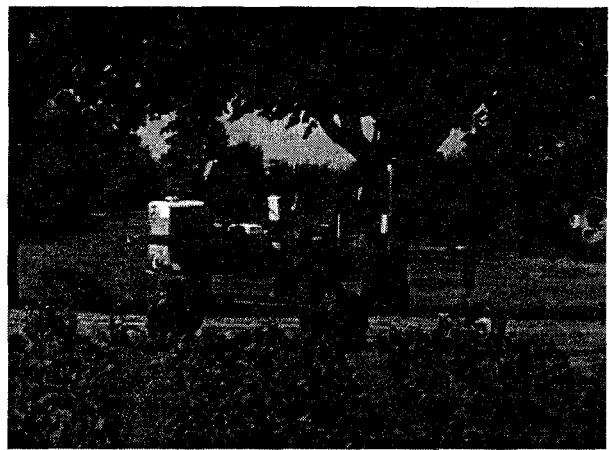
(a)



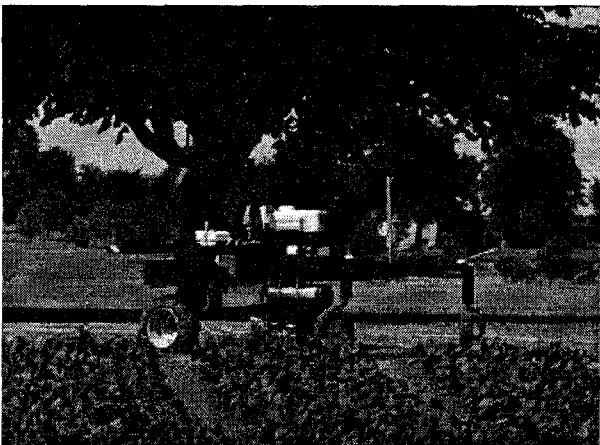
(d)



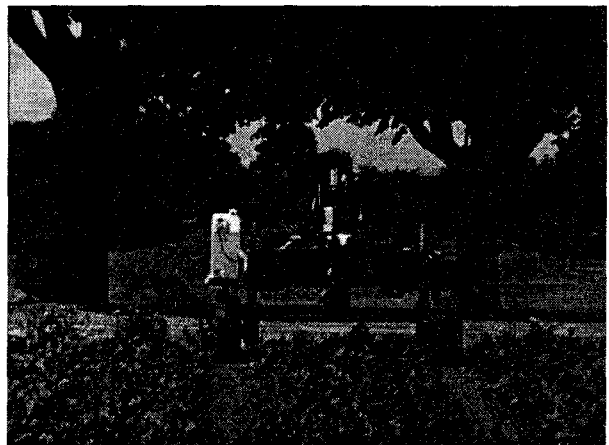
(b)



(e)



(c)



(f)

Figure 3: The vehicle executing a turning manoeuvre.